

Electronic Supplementary Information

**Renewable Conjugated Acids as Green Curatives for
High Performance Rubber/silica Composites**

Tengfei Lin, Xuhui Zhang, Zhenghai Tang, Baochun Guo*

Department of Polymer Materials and Engineering, South China University of
Technology, Guangzhou, 510640, P. R. China.

Content

1. Materials.....	2
2. Preparation of Model Compounds.....	2
3. Preparation of cured ENR composites.....	3
4. Characterization.....	3
5. ¹³ C NMR, ¹ H NMR and FTIR spectra of ENR gum.....	5
6. ¹³ C NMR and ¹ H NMR spectra of model compounds.....	7
7. Curing profiles of ENR vulcanizates.....	10
8. FTIR spectra of ENR vulcanizates.....	10
9. Morphology of ZnO.....	11
10. Morphology of ZDS-cured and ZDF-cured ENR.....	11
11. Mechanical properties of ENR vulcanizates.....	12
12. Storage modulus E' (left) and tan δ of ENR vulcanizates.....	13
13. Mechanical properties of the cured ENR/silica composites.....	14
14. Morphology of ENR/silica composites.....	15
15. References.....	16

1. Materials

ENR with an epoxidation degree of 50% was produced by the Agricultural Products Processing Research Institute, Chinese Academy of Tropical Agricultural Science, Zhanjiang, P. R. China. The structure for the ENR gum was first identified by ¹H, ¹³C NMR and FTIR spectroscopy (Figure S1 and Figure S2). SA (sorbic acid, chemically pure) and FA (ferulic acid, chemically pure) were purchased from Aladdin Industrial Corp., P. R. China. ZnO (zinc oxide, chemically pure) was purchased from Kemeng Chemical Industry & Trade Corp., P. R. China. The pristine ZnO crystals were hexagonal prisms with a primary particle diameter in the range of 100 to 500 nm according to SEM observations (Figure S7). Other rubber additives were industrially available products that were used as received. Precipitated silica (trade name VN3, nanosized silica, hereafter referred to as nanosilica) with a specific surface area of ~175 m²/g was purchased from Evonik Degussa Co., Ltd..

2. Preparation of Model Compounds

To reveal the reaction between hydroxyl groups and the conjugated double bonds of SA or FA, excessive 2,3-butanediol was reacted with ethyl sorbate or ethyl 3-(4-hydroxy-3-methoxyphenyl) acrylate (weight ratio of 5), which act as the analogues of the zinc salts of SA and FA, respectively. These reactions were catalysed by a trace amount of triphenylphosphine. The reaction was conducted under vigorous stirring at 45°C. The reaction was allowed to proceed for more than 72 h. After the heterogeneous reaction ended, the unreacted 2,3-butanediol was removed by vacuum-assisted evaporation. The obtained model compound was subjected to further characterization.

3. Preparation of cured ENR composites

ENR with a various amounts of ZnO and SA or FA were mixed using an open two-roll mill. The mole ratio between SA or FA and ZnO was fixed at 2:1. The well-mixed compounds were press-cured into 1 mm-thick sheets at 160°C for ~30 min. The sample names EZDS- χ and EZDF- χ denote a compound with χ phr SA and FA (relative to 100 parts of ENR), respectively. For comparison, ENR vulcanizate (hereafter denoted ES) was also cured using the traditional sulphur-curing package. The formulation was ZnO 4 phr, stearic acid 2 phr, N-cyclohexyl-2-benzothiazole sulphonamide (CZ) 1.5 phr, 2,2'-dibenzothiazole disulphide (DM) 0.5 phr, N-isopropyl-N'-phenyl-*p*-phenylene diamine (4010NA) 2 phr and sulphur 1.5 phr.

To further improve the properties of the ZDS-cured and ZDF-cured ENR, nanosilica was incorporated in the current formulation as a reinforcing material. The sample names EZDSSi- χ and EZDFSi- χ denote a compound with χ phr nanosilica and a fixed amount of 5 phr of the crosslinking agent (relative to 100 parts of ENR). For comparison, sulphur-cured ENR/silica composites (hereafter denoted ESSi30) with 30 phr nanosilica were also fabricated.

4. Characterization

Solvents and reagents were used as received. The ENR gum, reagents and model compounds were characterized by ^1H and ^{13}C NMR spectroscopy. ^1H NMR and ^{13}C NMR spectra were recorded on a Bruker AVANCE III 400 MHz spectrometer (400 MHz ^1H , 100 MHz ^{13}C) for samples dissolved in CDCl_3 containing TMS as an internal standard. Chemical shifts are reported in parts per million (ppm).

Tensile, tear, and hardness tests of the vulcanizates were performed at 25°C according to standards ISO 37-2005, ISO 34-2004 and ISO 7619-2004, respectively. Heat/oxygen

ageing was conducted in an age-circulating oven (GT-7017-NL) at 100°C for 7 days according to ASTM D 573.

The crosslink density was determined by the equilibrium swelling method in toluene and subsequently calculated according to the classical Florye–Rehner equation.¹ Briefly, the samples were swollen in toluene at room temperature for 72 h. The swollen samples were then removed from the solvent, and the surface toluene was quickly blotted off. The samples were immediately weighed, dried in a vacuum oven for 36 h at 80°C to remove all of the solvent and then reweighed. The volume fraction of ENR in the swollen gel, V_r , was calculated according to the following equation.²

$$V_r = \frac{m_0 \times \phi \times (1 - \alpha) / \rho_r}{m_0 \times \phi \times (1 - \alpha) / \rho_r + (m_2 - m_1) / \rho_s}$$

where m_0 is the sample mass before swelling, m_1 and m_2 are the sample masses before and after drying, respectively, ϕ is the mass fraction of rubber in the vulcanizate, α is the mass loss of the gum ENR vulcanizate during swelling, and ρ_r and ρ_s are the rubber and solvent densities, respectively.

The elastically active network chain density, V_e , which was used to represent the crosslink density, was then calculated by the well-known Flory–Rehner equation¹.

$$V_e = - \frac{\ln(1 - V_r) + V_r + \chi V_r^2}{V_s (V_r^{1/3} - V_r/2)}$$

where V_r is the volume fraction of the polymer in the vulcanizate swollen to equilibrium, V_s is the solvent molar volume (107 cm³/mol for toluene), and χ is the rubber–toluene interaction parameter and is taken as 0.0653 according to previous work.³

Dynamic mechanical analysis (DMA) was performed with a TA Q800 dynamic mechanical analyser (USA). The tests were carried out under the tension condition and at a frequency of 1 Hz. The scanning temperature ranged from -100 to 100°C at a heating rate of 5°C/min.

Fourier-transform infrared spectroscopy (FTIR) was performed on a Bruker Vertex 70 FTIR spectrometer with the samples in KBr pellets.

Akron abrasion tests were carried out on an Akron abrader (GT-7012-A, Gotech Testing Machines Co., Ltd., Taiwan). The slip angle was 15°, and the rotational speed of the abrader was 76 rpm under a loading of 26.7 N. All the specimens were pre-abraded for 600 revolutions before testing. The weight loss was recorded after a specified number of revolutions (the whole trip was 1.61 km, 3418 revolutions) of the abrasive wheel. The abrasion resistance of the specimen was calculated from its volume loss in terms of its weight loss and the rubber's density. Akron abrasion tests were repeated at least three times to ensure reproducibility. The cryogenically fractured surfaces and the abraded surfaces of the samples were observed by scanning electron microscopy (SEM) with a Hitachi S-4800 FESEM (Japan). The surfaces were plated with a thin layer of gold before the observation.

5. ¹³C NMR, ¹H NMR and FTIR spectra of ENR gum

The ENR gum was characterized by ¹³C NMR, and ¹H NMR; the results are presented in Figure S1. The assignments of the ¹³C NMR chemical shifts (δ , ppm) for ENR include CDCl₃, C₁, 134.85; C₂, 125.15; C₇, 64.52; C₆, 60.81; C₃, C₄, C₈, C₉, 33.08-23.85; C₅, 23.31; C₁₀, 22.23. For the ¹H NMR signals, the assignments of the chemical shifts for ENR include CDCl₃, H_a, 5.19; H_e, 2.74; H_b, H_c, 2.18-2.08; H_d, 1.72; H_f, H_g, 1.62; H_h, 1.32. The FTIR spectrum of pure ENR is shown in Figure S2. The peaks at 3000–2800 cm⁻¹ indicate the presence of methyl and methylene groups. The peaks at 1644 cm⁻¹ and 876 cm⁻¹ are assigned to the C=C bonds and epoxy groups, respectively. Additional peaks at approximately 1113–1064 cm⁻¹ indicate the presence of cyclic ether. The observed characteristic peaks were consistent with those reported in previous works.^{4,5}

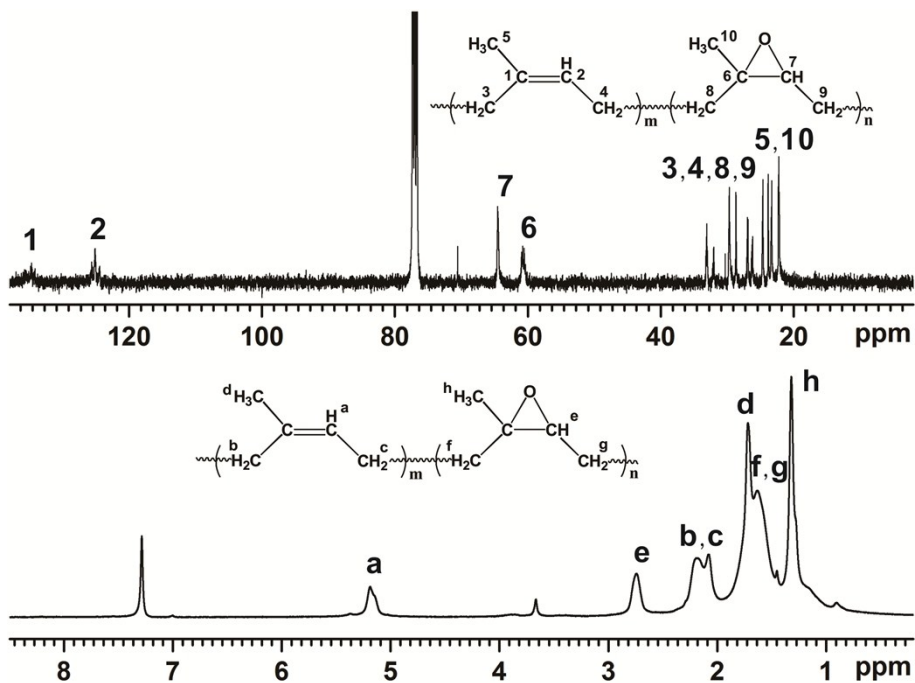


Figure S1. ^{13}C and ^1H NMR spectra of ENR gum.

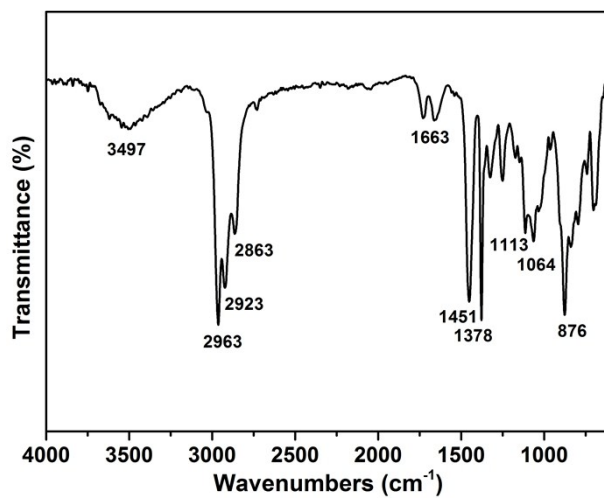


Figure S2. FTIR spectrum of ENR gum.

6. ¹³C NMR and ¹H NMR spectra of model compounds

The model compounds were characterized by ¹³C NMR and ¹H NMR; the results are presented in Figure S3 and Figure S4, respectively. The ¹³C NMR chemical shifts (δ , ppm) for the reactants were assigned first. These assignments include ethyl sorbate⁶ (CDCl₃, C₃, 166.67; C₄, 144.39; C₅, 138.56; C₆, 129.64; C₇, 118.84; C₈, 59.56; C₉, 18.10; C₁₀, 13.87), ethyl 3-(4-hydroxy-3-methoxyphenyl) acrylate⁷ (CDCl₃, C₃, 167.35; C₄, 148.12; C₅, 146.97; C₆, 144.87; C₇, 127.04; C₈, 123.05; C₉, 115.57; C₁₀, 114.83; C₁₁, 109.45; C₁₂, 60.47; C₁₃, 56.03; C₁₄, 14.29) and 2,3-butanediol⁸ (CDCl₃, C₁ and C₂, 70.65 and 16.80). The assignments of the carbons in the model compound were also made in the ¹³C NMR spectra. A comparison of the spectra of model compound (I) shows that the most significant characteristic was the emergence of new signals at approximately 69.41/74.10 ppm and 8.49/6.15 ppm, which are attributed to the carbon atom attaching to the ether (C₅'/C₁₁') and methyl (C₉'/C₁₂'), respectively.^{9, 10} In the case of the spectra of the model compound (II), the characteristic peaks at approximately 74.32/69.39 ppm and 18.07/7.05 ppm are attributed to the carbon atom attaching to the ether (C₆'/C₁₅') and methyl or methylene (C₉'/C₁₆'), respectively.

For the signals in ¹H NMR spectrum, the assignments of the chemical shifts for ethyl sorbate¹¹ (CDCl₃, H_d, 7.04; H_e, 5.94; H_f, 5.56; H_g, 3.98; H_h, 1.62; H_i, 1.07), ethyl 3-(4-hydroxy-3-methoxyphenyl) acrylate⁷ (CDCl₃, H_d, 7.64; H_e, 7.07; H_f, 7.02; H_g, 6.93; H_h, 6.31; H_j, 4.27; H_k, 3.90; H_l, 1.34) and 2,3-butanediol⁸ (CDCl₃, H_a, 4.14; H_b, 3.54; H_c, 0.91) were also first identified. For the ¹H NMR spectrum of the model compounds, the most important features, apart from the above mentioned signals, were the emergence of the signal for the ether-related hydrogen atoms. For the model compound (I), the signals at approximately 3.54–3.50 ppm were assigned to the hydrogen atoms neighboring ether (H_d' and H_m'). For the model compound (II), the signals of the hydrogens neighbouring ether (H_d' and H_m') were located at approximately 3.78 and 3.44 ppm. The ether moieties

were thus identified in the model compound. Therefore, both the ^{13}C and ^1H NMR results convincingly demonstrate the oxa-Michael addition between 2,3-butanediol and ethyl sorbate or ethyl 3-(4-hydroxy-3-methoxyphenyl) acrylate, which provides strong evidence for the cross-linking of ENR by the salts of SA or FA via an oxa-Michael reaction.

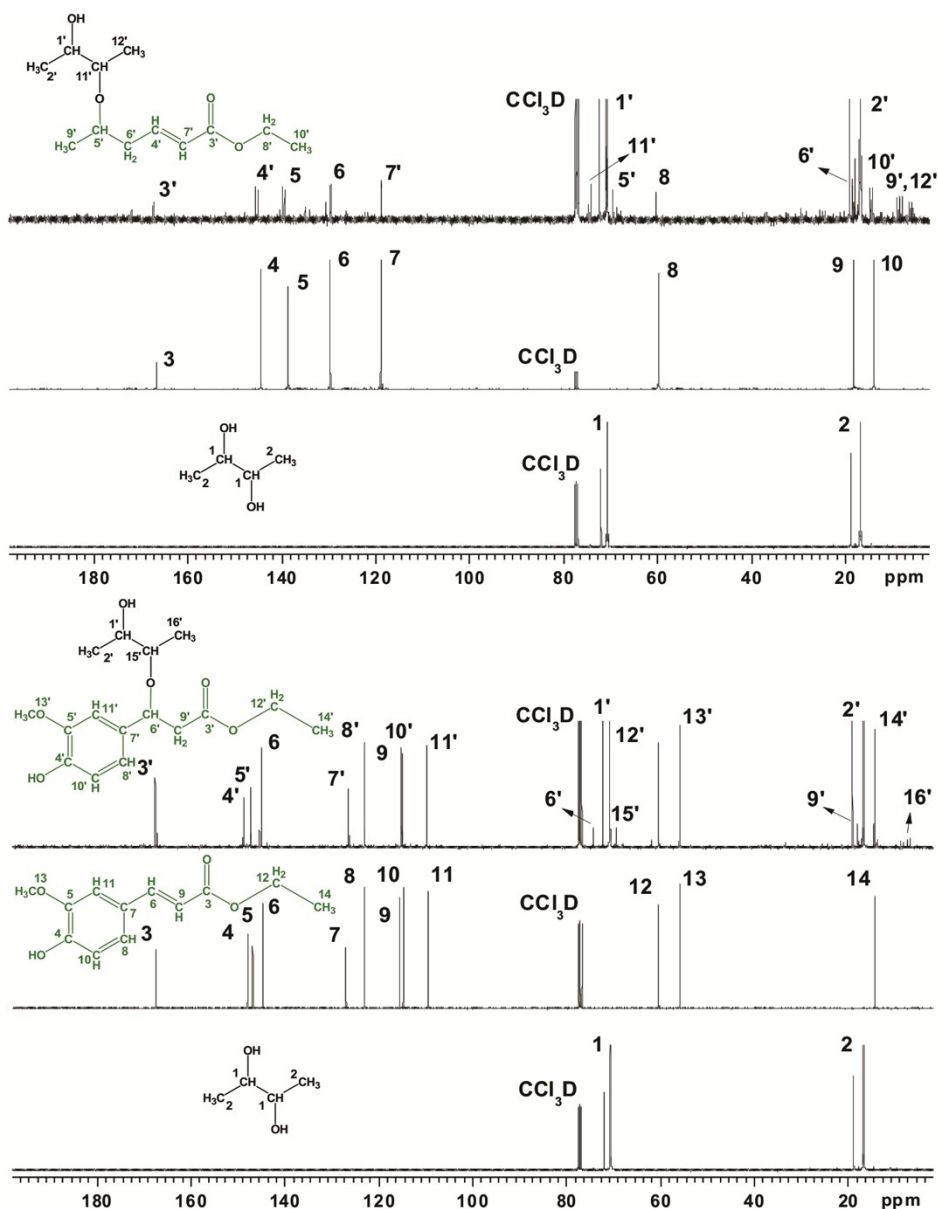


Figure S3. ^{13}C NMR spectra of 2,3-butanediol, ethyl sorbate, ethyl 3-(4-hydroxy-3-methoxyphenyl) acrylate, and their reaction product.

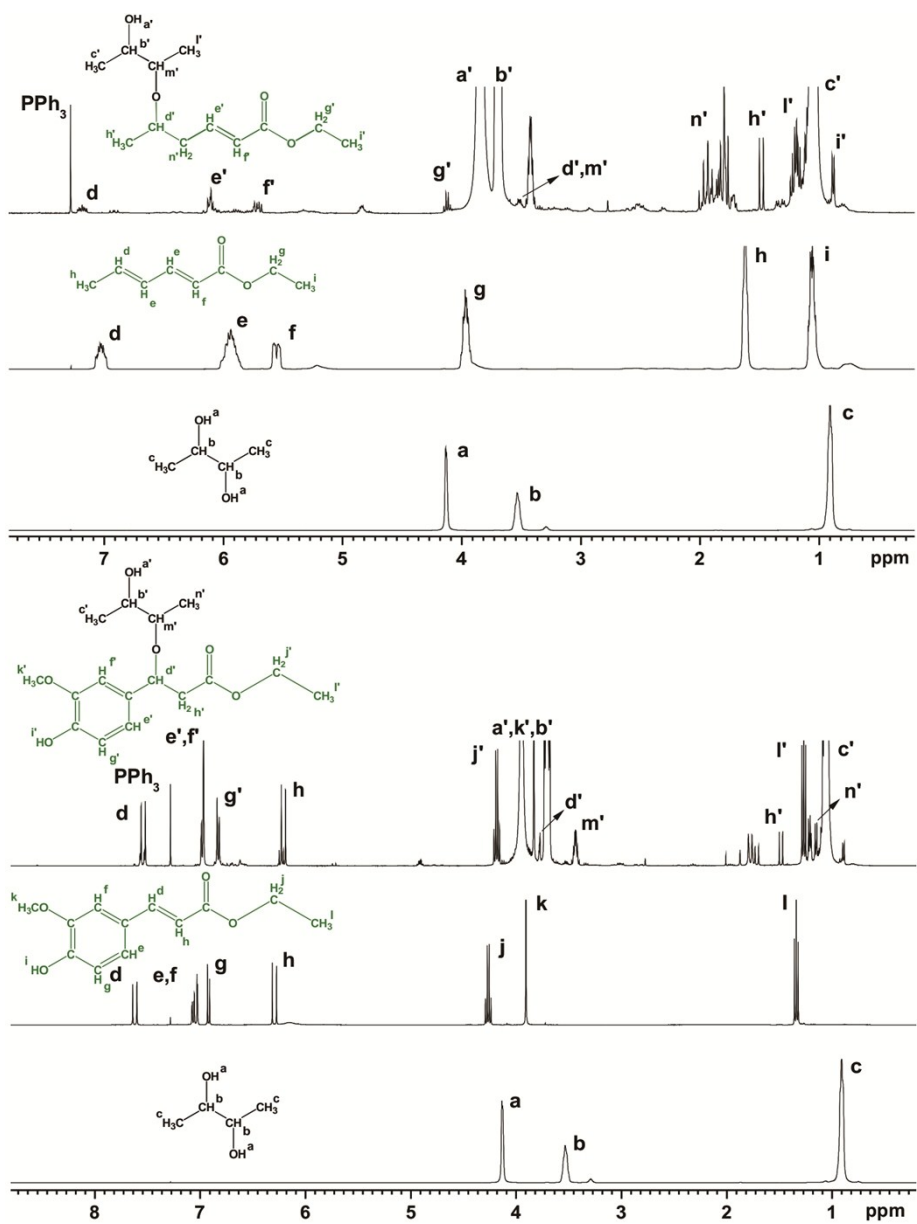


Figure S4. ^1H NMR spectra of 2,3-butanediol, ethyl sorbate, ethyl 3-(4-hydroxy-3-methoxyphenyl) acrylate, and their reaction product.

7. Curing profiles of ENR vulcanizates

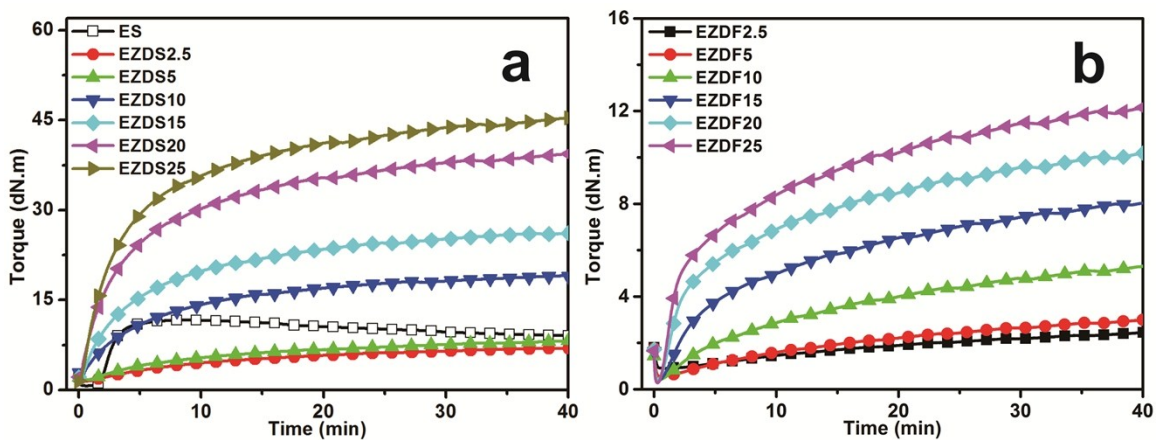


Figure S5. Profiles of the ENR curing via (a) ZDS and (b) ZDF.

8. FTIR spectra of ENR vulcanizates

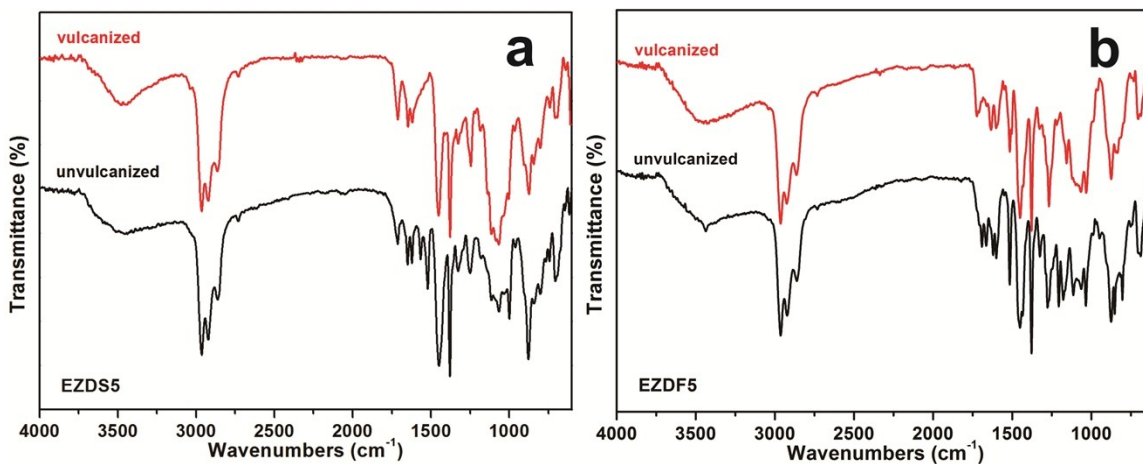


Figure S6. Comparison of the FTIR spectra of ENR vulcanizates before and after curing via (a) ZDS and (b) ZDF.

9. Morphology of ZnO

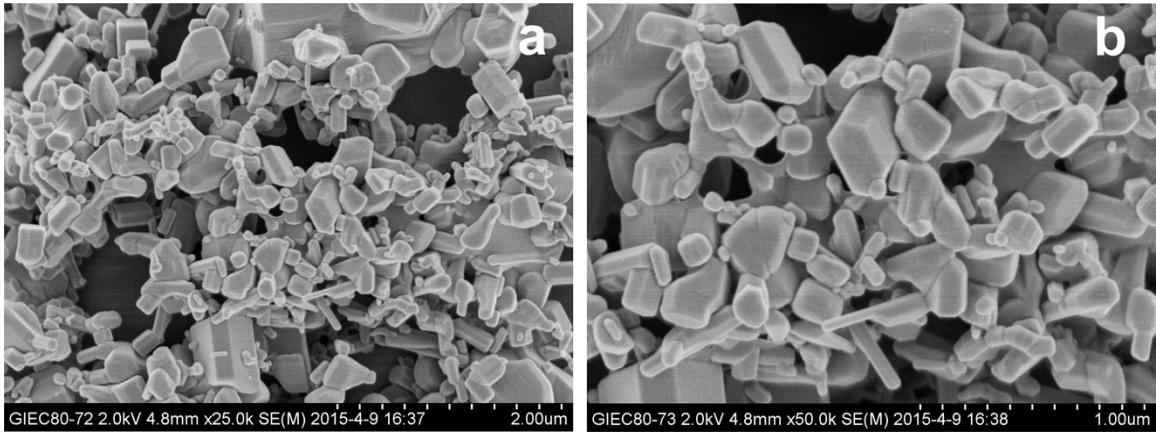


Figure S7. SEM images of ZnO powders.

10. Morphology of ZDS-cured and ZDF-cured ENR

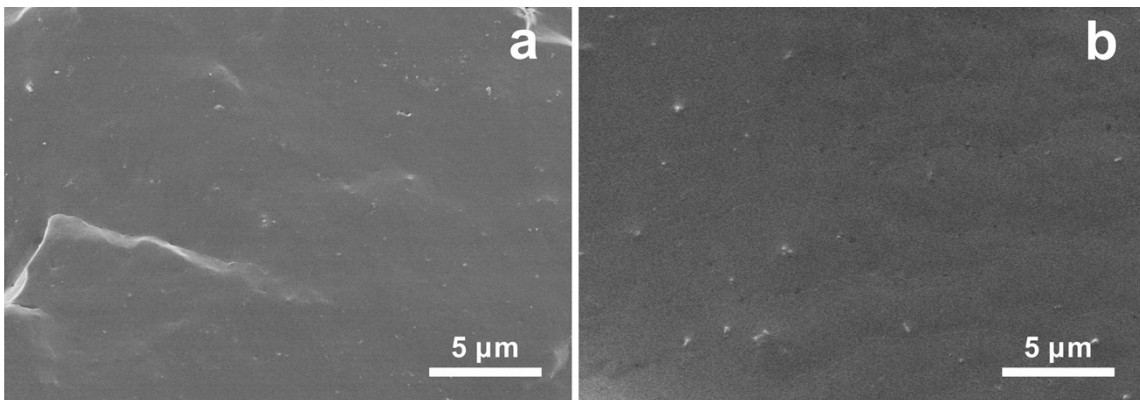


Figure S8. SEM images of (a) ZDS-cured and (b) ZDF-cured ENR.

11. Mechanical properties of ENR vulcanizates

Table S1. Mechanical properties of ENR vulcanizates.*

Sample	Tensile strength (MPa)	Strain at break (%)	Modulus at 300% strain (MPa)	Permanent set (%)	Tear strength (kN.m ⁻¹)	Shore A hardness
ES	27.6±1.9	636±5	2.7±0.2	14	18.7±0.5	46
EZDS2.5	4.1±0.4	461±31	2.2±0.1	1	12.6±0.7	40
EZDS5	6.8±0.8	432±24	3.6±0.2	2	16.4±1.4	46
EZDS10	7.3±0.8	407±40	5.4±0.2	6	21.4±2.9	53
EZDS15	11.7±0.8	449±12	6.4±0.1	11	25.5±0.8	64
EZDS20	13.2±1.3	413±17	8.6±0.2	14	30.7±2.5	69
EZDS25	13.5±1.3	416±23	9.6±0.9	22	31.2±1.4	72
EZDF2.5	3.0±0.5	722±16	1.1±0.1	3	7.7±0.3	33
EZDF5	3.0±0.4 ^N	586±33	1.2±0.1	1	8.4±1.0 ^N	39
EZDF10	7.6±0.7	576±37	2.3±0.1	4	13.7±0.5	45
EZDF15	11.7±0.5	583±6	3.3±0.2	6	17.4±1.1	51
EZDF20	10.8±1.4	516±13	4.2±0.3	10	18.5±0.3	58
EZDF25	12.4±1.0	471±16	6.8±0.3	13	30.9±3.5	68

* For most case, the tensile strength, modulus at 300% strain and tear strength of ENR vulcanizates are statistically different with increasing ZDS or ZDF loading ($P<0.05$); N presents not statistically significantly different ($P>0.05$); paired t-test, n=5.

12. Storage modulus E' (left) and $\tan \delta$ of ENR vulcanizates

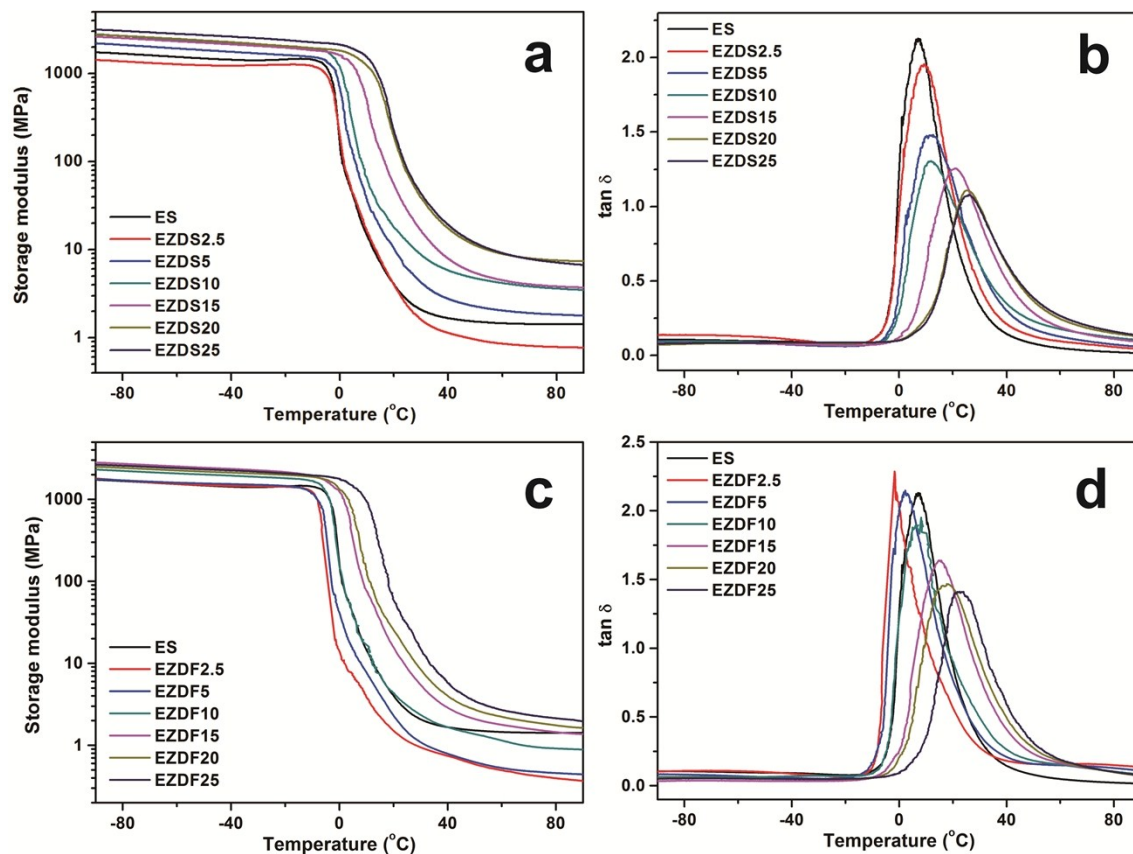


Figure S9. Storage modulus E' (left) and $\tan \delta$ (right) of the ZDS-cured and ZDF-cured ENR.

13. Mechanical properties of the cured ENR/silica composites

Table S2. Mechanical properties of the ENR/silica composites.*

Sample	Tensile strength (MPa)	Strain at break (%)	Modulus at 100% strain (MPa)	Permanent set (%)	Tear strength (kN.m ⁻¹)	Shore A hardness
ESSi30	21.3±2.4	491±45	2.4±0.1	19	29.7±1.4	58
EZDSSi10	11.3±1.2	495±26	1.4±0.1 ^N	3	19.7±2.2 ^N	45
EZDSSi20	11.4±1.0	413±24	1.9±0.1	2	18.3±1.7 ^N	48
EZDSSi30	15.2±2.1	296±30	4.5±0.3	4	23.0±1.2	64
EZDSSi40	13.2±1.2	248±25	5.1±0.8	4	36.6±1.4	67
EZDFSi10	6.5±0.4	624±19	1.1±0.1	4	13.0±0.6	42
EZDFSi20	9.1±0.3	521±16	1.8±0.2	8	19.9±0.7	55
EZDFSi30	12.3±1.2	389±22	3.8±0.2	11	30.9±1.7	68
EZDFSi40	14.6±1.4	356±38	5.5±0.2	17	35.7±2.3	83

* For most case, the tensile strength, modulus at 100% strain and tear strength of the ENR/silica composites are statistically significantly different with increasing nanosilica loading ($P<0.05$); N presents not statistically significantly different ($P>0.05$); paired t-test, n=5.

14. Morphology of ENR/silica composites

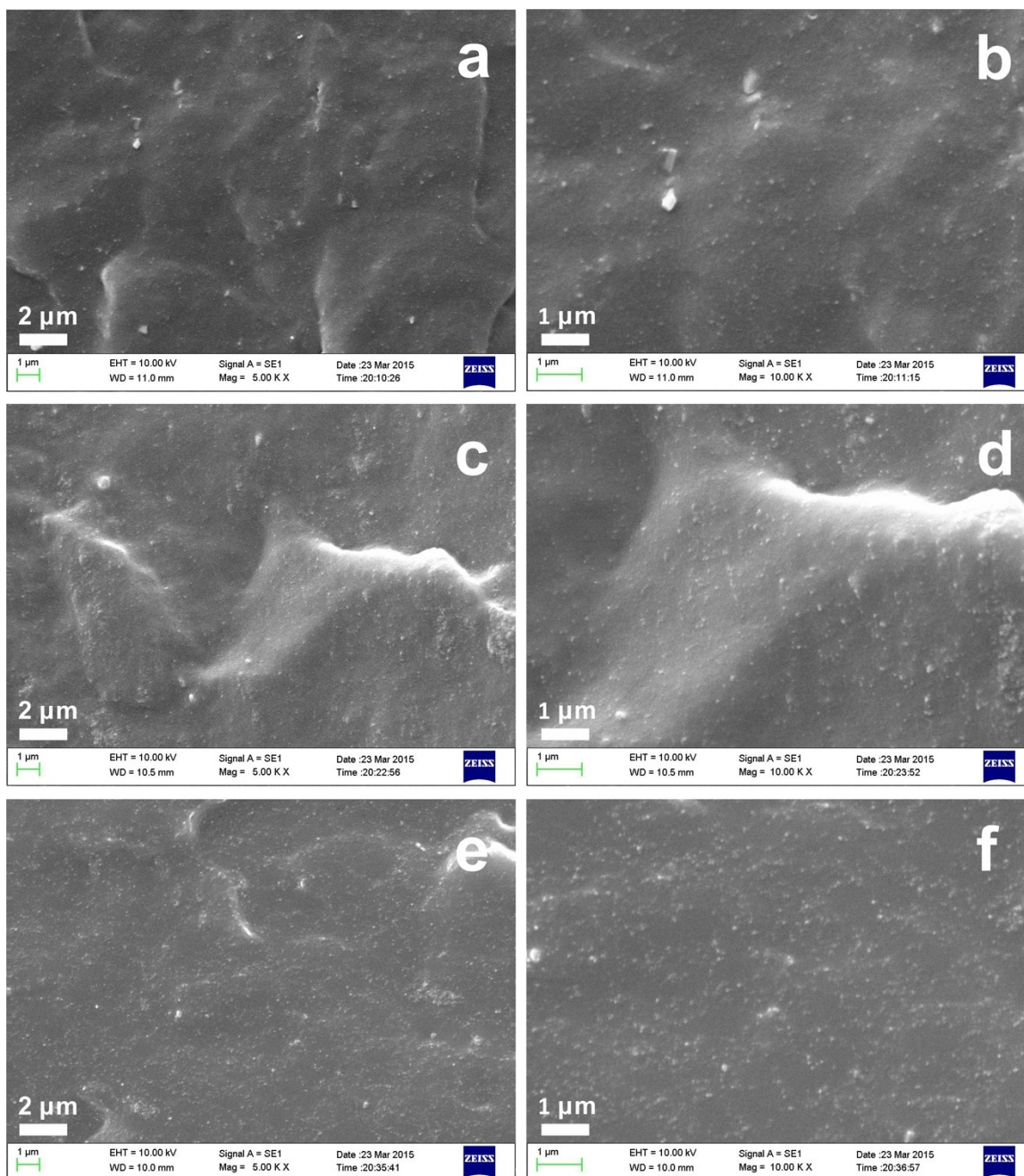


Figure S10. SEM images of (a, b) sulphur-cured, (c, d) ZDS-cured and (e, f) ZDF-cured ENR/silica composites.

References

1. P. J. Flory, *J. Chem. Phys.*, 1950, **18**, 108-111.
2. P. J. Flory and J. J. Rehner, *J. Chem. Phys.*, 1943, **11**, 521-526.
3. C. Sheehan and A. Bisio, *Rubber Chem. Technol.*, 1966, **39**, 149-192.
4. R. Hamzah, M. A. Bakar, M. Khairuddean, I. A. Mohammed and R. Adnan, *Molecules*, 2012, **17**, 10974-10993.
5. T. Saito, W. Klinklai and S. Kawahara, *Polymer*, 2007, **48**, 750-757.
6. L. Bollans, J. Bacsá, J. A. Iggo, G. A. Morris and A. V. Stachulski, *Org. Biomol. Chem.*, 2009, **7**, 4531-4538.
7. C. Vafiadi, E. Topakas, K. K. Wong, I. D. Suckling and P. Christakopoulos, *Tetrahedron: Asymmetry*, 2005, **16**, 373-379.
8. S. Mehta, G. Ram, R. Chauhan and K. Bhasin, *J. Chem. Thermodyn.*, 2009, **41**, 1329-1338.
9. G. R. Fulmer, A. J. M. Miller, N. H. Sherden, H. E. Gottlieb, A. Nudelman, B. M. Stoltz, J. E. Bercaw and K. I. Goldberg, *Organometallics*, 2010, **29**, 2176-2179.
10. H. E. Gottlieb, V. Kotlyar and A. Nudelman, *J. Org. Chem.*, 1997, **62**, 7512-7515.
11. J. Wu and C. Yue, *Synth. Commun.*, 2006, **36**, 2939-2947.